

Supporting information

Facile and template-free fabrication of hierarchical coral spheres for acetone gas sensor

Ying Liu,^a Baoteng Li,^a Sailong Xu,^{*a} Ying Guo^{* a}

^a State Key Laboratory of Chemical Resource Engineering, Beijing University of Chemical Technology,

P. O. 98, Beijing 100029, P.R.China. E-mail: guoying@mail.buct.edu.cn

As shown in Fig. S1 (a-b), the addition of sodium citrate and ammonium fluoride resulted in the formation of the unique coral spheres structure in ZnO material. Fig. S1 (c-d) shows that when only ammonium fluoride was added without sodium citrate, the ZnO material formed a sheet-like morphology, indicating that sodium citrate played a chelating agent role in the formation of coral spheres morphology. As shown in Fig. S1 (e-f), when ammonium fluoride was not added and only sodium citrate was added, the main morphology structure of ZnO material was spherical, and the surface of the spherical shape is sheet-like, indicating that ammonium fluoride acted as a structural guiding agent. Therefore, the formation of the unique morphology of ZnO coral spheres is attributed to the synergism of sodium citrate and ammonium fluoride. Sodium citrate acts as a complexing agent in the formation of spherical morphology of coral spheres, while ammonium fluoride acts as a structural directing agent. Without anyone of them, the coral sphere can not be obtained.

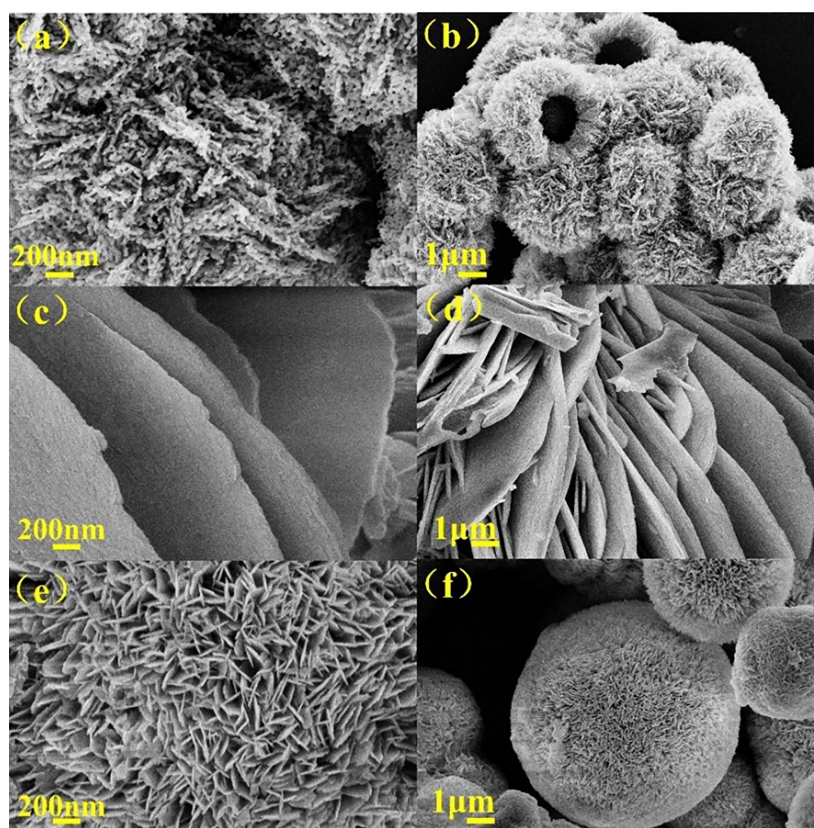


Fig. S1. SEM images of (a) ZnO coral spheres with ammonia fluoride and sodium citrate added together, (c-d) ZnO nanosheets without adding sodium citrate, (e-f) ZnO coral spheres without adding ammonia fluoride.

Fig. S2 shows the morphologies of ZnO, CeO₂/ZnO-1, CeO₂/ZnO-3, CeO₂/ZnO-4 coral spheres. It can be observed that the morphologies of all as-synthesized samples are similar, and no other different morphologies are observed, indicating a small amount of CeO₂ could not affect the morphology of ZnO sample. And the diameters of the ZnO, CeO₂/ZnO-1, CeO₂/ZnO-3, CeO₂/ZnO-4 coral spheres range from 7 to 10 μm. In addition, the obtained ZnO and CeO₂/ZnO coral spheres are constructed by numerous primary nanoparticles. During the reaction, numerous primary nanoparticles aggregate and assemble into coral structure, meanwhile, with the help of citrate sodium, the coral structure can further assemble into coral spheres structure. The unique coral sphere structure of the materials has a large specific surface area and provides sufficient

adsorption sites for gas molecules.

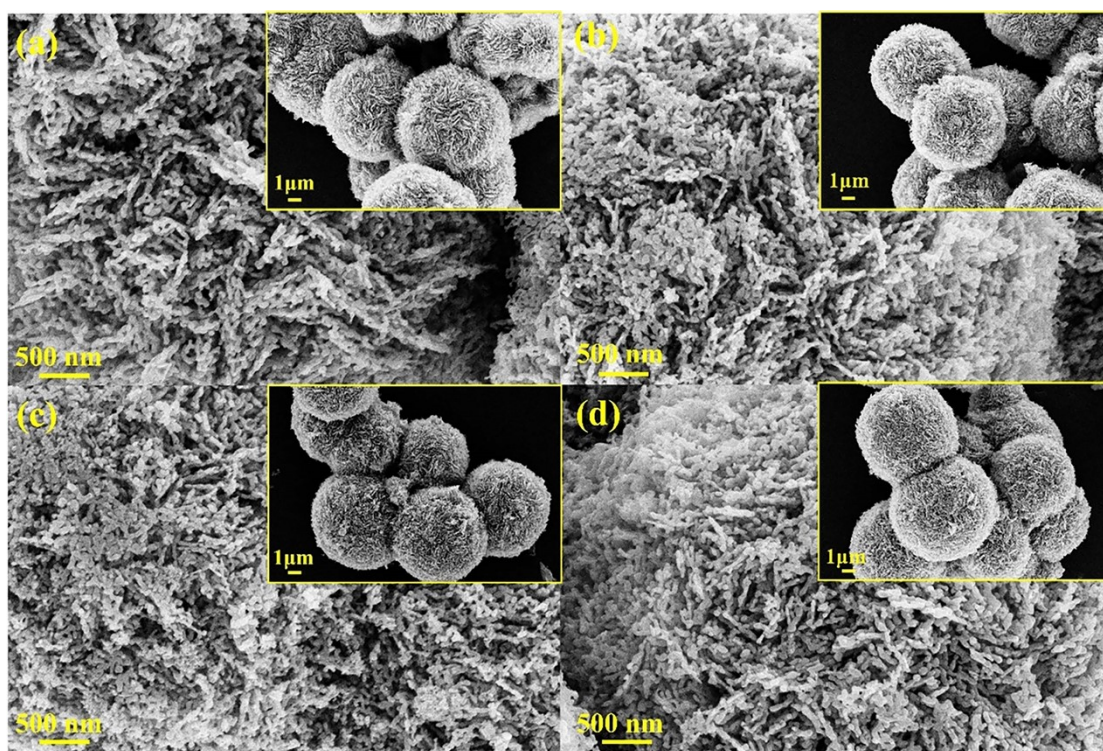


Fig. S2. SEM images of (a) ZnO; (b) CeO₂/ZnO-1; (c) CeO₂/ZnO-3; (d) CeO₂/ZnO-4 coral spheres.

As shown in Fig.S3 (a-d), when the calcination temperature is 450°C and 550°C, the surface of coral spheres is mostly stacked with flake particles, and the spherical shape is not as regular as that of coral spheres calcined at 500°C. When the calcination temperature was raised to 650°C, the obtained material no longer possesses the structure of coral spheres, and serious sintering occurred. Therefore, the calcination temperature was set to be 500 °C for the subsequent research.

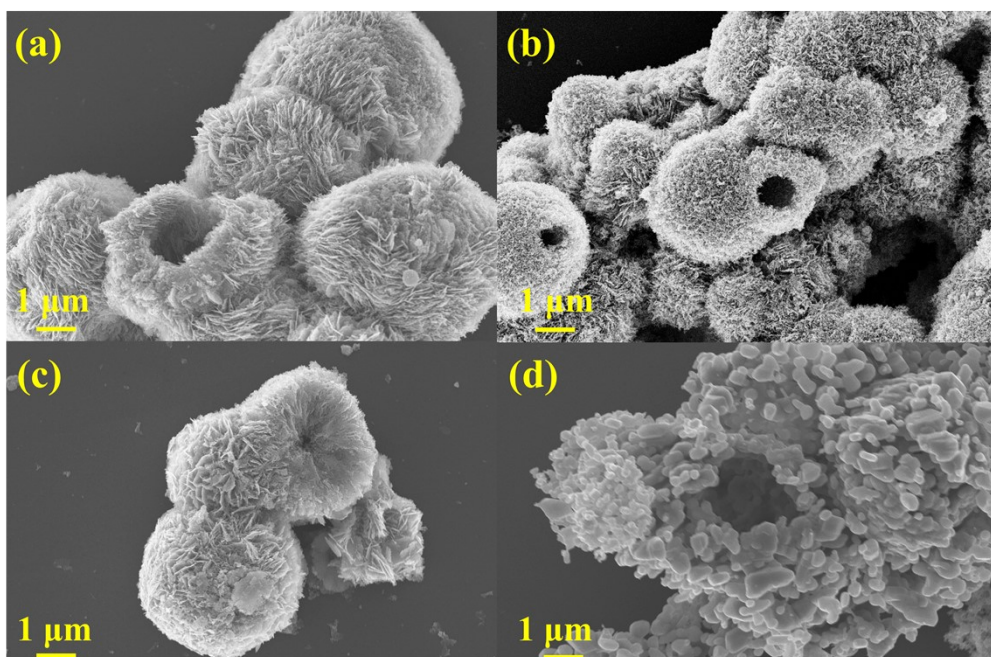


Fig. S3. SEM images of CeO₂/ZnO-2 coral spheres obtained at different calcination temperatures (a) 450°C, (b) 500°C, (c) 550°C, (d) 650°C.

Fig. S4 and Fig. S5 show the resistance response and recovery curves of CeO₂/ZnO-2 sensor to 10-800 ppm acetone at 245°C. Although CeO₂/ZnO-2 sensor shows the highest response at 215°C, the practical application of sensors must be considered for sensitivity, working temperature, response time and recovery time, etc. Therefore, the recovery time of CeO₂/ZnO-2 sensor along with the working temperature was further investigated. As shown in Fig. S6a and S6b, it could be seen that the response value of CeO₂/ZnO-2 sensor is 202 and the response time is 16 s at 215°C. While the recovery time of CeO₂/ZnO-2 sensor is 540 s at 215°C, which is very long. Although the response value of CeO₂/ZnO-2 sensor is the highest at 215°C, it is not practical due to its long recovery time at this working temperature. Hence, it is not a suitable working temperature for CeO₂/ZnO-2 sensor. As shown in Fig. S6c and S6d, the response value of CeO₂/ZnO-2 sensor is 143 and the response time and recovery

time are 16 s and 240 s at 245°C, respectively. At 245°C, CeO₂/ZnO-2 sensor still shows enhanced response value to acetone as compared to ZnO sensor and the optimum working temperature of CeO₂/ZnO-2 sensors is still lower than that of ZnO sensor. Hence, considering the factors of the sensitivity and the recovery time, the optimum working temperature of CeO₂/ZnO-2 sensor was set at 245°C for future investigation.

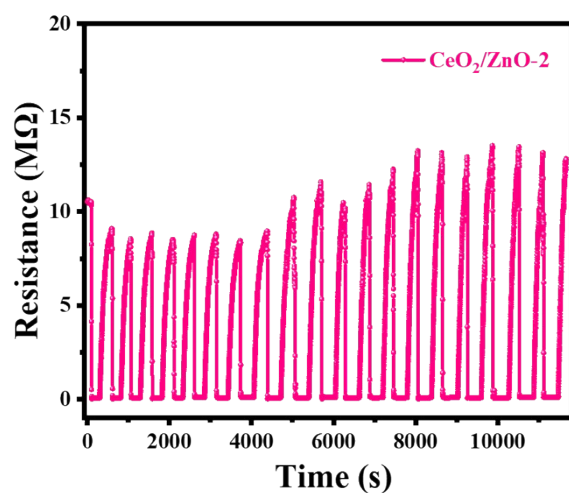


Fig. S4. Resistance response and recovery curves of CeO₂/ZnO-2 sensor to 100 ppm acetone at 245°C.

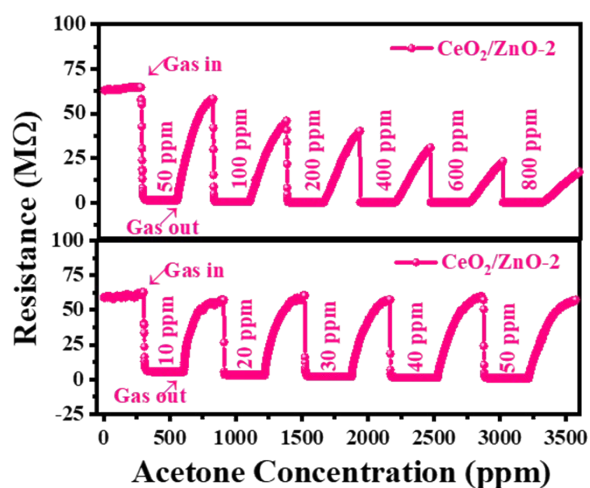


Fig. S5. Resistance response and recovery curves of CeO₂/ZnO-2 sensor to 10-800 ppm acetone at 245°C.

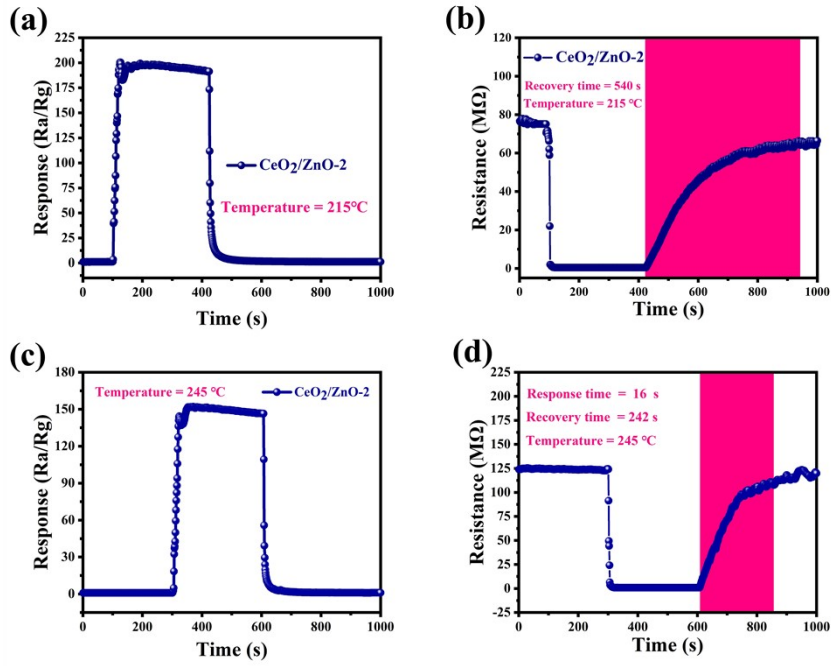


Fig. S6.; (a) Response and recovery curve of CeO₂/ZnO-2 sensor to 100 ppm acetone at 215°C; (b) Resistance curve of CeO₂/ZnO sensor to 100 ppm acetone at 215°C; (c) Response and recovery curve of CeO₂/ZnO-2 sensor to 100 ppm acetone at 245°C; (d) Resistance curve of CeO₂/ZnO-2 sensor to 100 ppm acetone at 245°C.

As shown in Table S1, the response time and recovery time of CeO₂/ZnO-2 sensors to acetone gas were compared with the other three groups of sensors. It can be seen that the CeO₂/ZnO-2 sensor has the shortest response and recovery time for acetone gas sensing.

Table S1. Comparison of response time and recovery time of CeO₂/ZnO sensors at 245°C.

Sensor	Response time (s)	Recovery time (s)
CeO ₂ /ZnO-1	43	279
CeO ₂ /ZnO-2	16	242
CeO ₂ /ZnO-3	38	290
CeO ₂ /ZnO-4	49	302

As listed in Table S2, the acetone-sensing properties of the as-obtained CeO₂/ZnO-2 sensor are compared with other ZnO-based sensors. Considering the optimum working temperature and sensitivity, the CeO₂/ZnO-2 sensor exhibits a competitive performance in comparison with other ZnO-based sensors toward acetone gas. From the above results, it is believed that the CeO₂/ZnO-2 sensor has potential for detecting the acetone gas.

Table S2. Comparison of gas-sensing performance of acetone sensors based on ZnO.

Materials	Temperature (°C)	Concentration (ppm)	Response (Ra/Rg)	References
Fe-ZnO porous nanosheets	350	100	105.7	Mater. Sci. Semicond. Process., 2022, 148, 106807
ZnO/ZnFe ₂ O ₄	260	100	18.92	Ceram. Int., 2020, 46, 5960-5967
ZnO@CeO ₂ nanofibers	370	1	8.2	Ceram. Int., 2019, 45, 4103-4107
CeO ₂ /ZnO composite	320	5	16.2	Funct. Mater. Lett., 2020, 13, 2050013-2050017.
5Pt/ZnO	190	100	47.7	Mater. Lett., 2021,304, 130682-130682
Ni-ZnO maize straw	340	100	68	Sens. Actuators, B, 2017, 243,1224-1230
α-Fe ₂ O ₃ /ZnO	300	50	45.25	ACS Appl. Nano Mater., 2022, 5, 5745–5755
Co ₃ O ₄ /ZnO	273	50	201	J. Mater. Sci.-Mater. Electron., 2023, 34, 128
Zn ₂ TiO ₄ -ZnO	370	100	33.4	Rare Matels, 2021, 40, 1528-1535
CeO ₂ /ZnO coral spheres	245	100	143	this work